

seismic phases, is not possible for core-diffracted waves because of the rapid loss of high frequencies during diffraction. A linear regression through the times of the wave peak maxima is the common means of determining the apparent slowness (18, 27) [J. C. Mondt, *Phys. Earth Planet. Inter.* 15, 46 (1977); A. Souriau and G. Poupinet, *ibid.* 84, 227 (1994)], and

this has been shown to be as reliable as using a multiwaveform cross-correlation [M. E. Wyssession and E. A. Okal, *Geophys. Res. Lett.* 16, 1417 (1989)].
 31. M. E. Wyssession, L. Bartkó, J. Wilson, *J. Geophys. Res.* 99, 13667 (1994).
 32. We thank the many people with the IRIS PASSCAL and DMC programs who helped with the MOMA

experiment and K. Koper, A. Li, E. Roth, L. Salvati, R. Valenzuela, and J. Zaslow for additional help with the MOMA deployment. Supported by NSF grants EAR-9319324, EAR-9315971, and EAR-9315925 and by the David and Lucile Packard Foundation.

14 October 1998; accepted 23 February 1999

High-Resolution Holocene Environmental Changes in the Thar Desert, Northwestern India

Y. Enzel,¹ L. L. Ely,² S. Mishra,³ R. Ramesh,⁴ R. Amit,⁵ B. Lazar,¹
 S. N. Rajaguru,³ V. R. Baker,⁶ A. Sandler⁵

Sediments from Lunkaransar dry lake in northwestern India reveal regional water table and lake level fluctuations over decades to centuries during the Holocene that are attributed to changes in the southwestern Indian monsoon rains. The lake levels were very shallow and fluctuated often in the early Holocene and then rose abruptly around 6300 carbon-14 years before the present (¹⁴C yr B.P.). The lake completely desiccated around 4800 ¹⁴C yr B.P. The end of this 1500-year wet period coincided with a period of intense dune destabilization. The major Harrapan-Indus civilization began and flourished in this region 1000 years after desiccation of the lake during arid climate and was not synchronous with the lacustral phase.

The southwestern Indian monsoon is critical for understanding past global and regional monsoon variations (1-3). The few records of Holocene monsoon variations from the areas that border the Arabian Sea in southern Asia have been based on pollen assemblages associated with the deposits of Lunkaransar, Didwana, and Sambhar paleolakes from northwestern India (4). These records, although based on limited dating, have been used extensively in regional compilations, in analysis of relations between summer insolation and the monsoon, and in paleoclimatic models (2-7) as well as to determine the relations between paleoclimate and Indus Valley civilizations (8, 9). Here, we present more detailed Holocene chronology of Lunkaransar based on analyses of the lacustrine laminated deposits, age dating, and geochemical analyses.

Lunkaransar (10) is a small, closed, dry basin surrounded by dunes at the northeastern margin of the Thar Desert (Fig. 1). The basin receives input from groundwater and direct rain

and no input from streams. The water table is currently 2.4 m below the dry lake bed, and this water is saline with a composition that includes Na, Ca, Mg, Cl, SO₄, and HCO₃. Incoming sediments are only eolian sand from local dunes and eolian clay silt dust (11). Normally, the lake basin is totally dry, but heavy rainfall can form a temporary pool of water that evaporates during the dry season.

Trenches were excavated into the lake bed down to a thick, hard, carbonate layer at a depth of 3 m. The sedimentology of the upper 240 cm above the water table (Fig. 2) was documented at submillimeter-to-millimeter scales in both the field exposures and in the continuous, overlapping box cores in the laboratory. We obtained 15 radiocarbon dates (Table 1). The sequence was divided into four zones (Fig. 2) on the basis of characteristics of the deposits. Zone 4, dated at 4800 ¹⁴C yr B.P. to recent, has no primary laminar structure and contains mud cracks, silt, and sand; it is interpreted as a dry lake basin that episodically was inundated by ephemeral lakes. Zones 1 to 3 (Figs. 2 and 3) are composed of two types of thin beds: (i) silt- and clay-rich detritus laminae with carbonate and in some cases thin gypsum laminae at boundaries, and (ii) gypsum laminae with some thin silt and clay laminae. We separated the entire sequence into four sedimentary facies (II to V) according to the dominant type and the thickness of the various beds (Fig. 3E) and inferred relative water depths

Field observations show that the maximum lake stage did not reach 5 to 7 m. The ability of the basin to sustain even this level (facies IV and V) through successive years varied significantly throughout the Holocene (Fig. 3E).

Thin-section and x-ray diffraction analyses indicate that the clastics are allochthonous silicate minerals (quartz, plagioclase, potassium feldspar, clays such as chlorite and mica, and some hornblende), carbonate minerals, and some gypsum. Gypsum is the only evaporite mineral detected. The clay fraction (<2 μm) includes illite-smectite, illite, chlorite, and palygorskite. The palygorskite is authigenic and is indicative of intense evaporation episodes (12) at pH ≈ 8.5.

The concentration of clastic grains in separate laminae and the parallel orientation of the platy and elongated minerals indicate that the clastic grains were derived from dust storms (11) and they settled in water. The gypsum laminae contain fine authigenic crystals and abraded, sand-sized gypsum crystals. The abraded gypsum grains are most common in facies II and were probably blown in from drying mudflats at the margins (13) of Lunkaransar lake during periods of low lake levels.

The rise and fall of the water table at Lunkaransar reflect the regional precipitation over the basin. A lake is formed in Lunkaransar when the water table rises above the surface. Our data show that between about

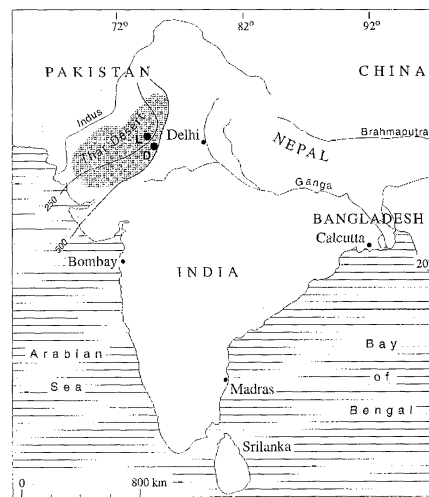


Fig. 1. Location map of Lunkaransar (L) and Didwana (D) dry lakes in the Thar Desert (shaded area) showing 250- and 500-mm/year isohyets.

¹Institute of Earth Sciences and Department of Geography, The Hebrew University of Jerusalem, Jerusalem 91904, Israel. ²Department of Geology, Central Washington University, Ellensburg, WA 98926, USA. ³Deccan College, Deccan College Road, Pune 411006, India. ⁴Earth Science Division, Physical Research Laboratory, Ahmedabad 380009, India. ⁵Geological Survey of Israel, 30 Malkhei Israel Street, Jerusalem, Israel. ⁶Department of Hydrology and Water Resources, University of Arizona, Tucson, AZ 85721, USA.

REPORTS

10,000 and 4800 ¹⁴C yr B.P. the lake did not dry, and therefore the water table was always above the basin floor. Since 4800 ¹⁴C yr B.P., the water table has been below the surface. Because of deposition in the basin, the elevation of the present-day water table at 2.4 m below the surface can be identical to the elevation of its levels during the low stands of the early Holocene lake. The early Holocene monsoon rains were not able to maintain a stable lake in this area for more than a few decades at a time, although there is no evidence of complete desiccation at any time before 4815 ± 75 ¹⁴C yr B.P. (Fig. 3E). The only period when a sustained high-lake stand is evident in this basin during the Holocene was from 6300 to 4800 ¹⁴C yr B.P. (zone 3) (Fig. 3E). Few to no evaporite layers exist between the silt laminae in the deposits from this period, indicating that the relatively high lake levels persisted year round and did not decline annually during the winter dry season, as is evident in other parts of the section where gypsum laminae alternate with each of the submillimeter clastic dust layers.

The values of δ¹³C of organic carbon (14) in the lake show two dramatic shifts during the

Holocene (Fig. 3A). δ¹³C_{org} decreased from -14 per mil to -20 per mil around 6300 ¹⁴C yr B.P. and returned abruptly at about 5500 to 5000 ¹⁴C yr B.P. (Fig. 3A). The sudden drop could reflect an abrupt increase in the relative abundance of C₃ versus C₄ vegetation transported into the lake during a period of increased precipitation. Such an explanation, however, implies an extremely rapid change in the regional environmental conditions of the Thar desert.

A more plausible explanation is that the δ¹³C_{org} within the lake itself changed. During its earlier history (before 6300 B.P.) the lake was likely a shallow pan covered by extensive microbial (algal) mats. Remnants of mats are evident in all parts of the Lunkaransar cores. Productive mats can deplete a shallow water column of its dissolved inorganic carbon (DIC)

(15). This depletion in turn drives an influx of atmospheric CO₂, which yields DIC with a negative (typically -6 per mil) δ¹³C value (15, 16). In deep water, the mat photosynthesis will not be able to deplete the DIC and the δ¹³C_{DIC} will rise. The commonly used proxy, the isotopic composition of CaCO₃ (δ¹³C_{carb}), is misleading in this case (Fig. 3B) because it represents mainly wind-blown carbonates, whereas δ¹³C_{org} represents genuine autochthonous organic matter (17). In this model, the time of maximum insolation of the early Holocene (<6300 ¹⁴C yr B.P.) is associated in Lunkaransar with rather high δ¹³C_{org}, representing mat growth in extremely shallow water (10 to 40 cm); the noticeable shift in δ¹³C_{org} at about 6300 ¹⁴C yr B.P. indicates, according to this model (18), a rise in lake level to >50 cm. The absence of gypsum at this zone (Fig. 2) sup-

Table 1. Lunkaransar radiocarbon analyses: s, sediment; c, charcoal. Calibration was done according to (22). PDB, Pee Dee belemnite standards.

Sample	Laboratory	Depth (cm)	Material dated	δ ¹³ C (per mil, PDB)	¹⁴ C date (yr B.P.)	Calibrated age (1σ) (yr B.P.)
LU-8	AA-11116	17 to 18	s	-17.4	2325 ± 65	2430 to 2160
LU-9	AA-22005	26 to 28	s	-16.8	3785 ± 75	4270 to 3990
LU-34	AA-28411	30	c	-24.7	4230 ± 55	4860 to 4650
LU-10	AA-11117	34.5 to 35.5	s	-20.7	4815 ± 75	5640 to 5460
LU-11	AA-11118	41 to 42	s	-17.2	5010 ± 100	5900 to 5640
LU-14	AA-22006	53.5 to 54.5	s	-13.8	6055 ± 60	7000 to 6810
LU-30	A-7302	61 to 67	s	-13.8	5925 ± 125	6900 to 6620
LU-18	AA-11121	71.5 to 72.5	s	-15.8	6235 ± 80	7210 to 7010
LU-19	AA-11122	78.7 to 79.7	s	-13.6	6300 ± 75	7270 to 7160
LU-24	AA-11123	142.5 to 144	s	-10.6	8375 ± 85	9450 to 9260
LU-31	A-7303	147 to 150.5	s	-12.8	8640 ± 80	9800 to 9490
LU-25	AA-11124	156 to 157.5	s	-14.1	8200 ± 80	9230 to 9000
LU-27	AA-11125	177 to 178.5	s	-13.9	8430 ± 90	9490 to 9360
LU-28	AA-11126	196 to 197	s	-13.4	9180 ± 85	10,280 to 10,040
LU-32	AA-12207	216 to 221	s	-13.8	9615 ± 75	10,910 to 10,570

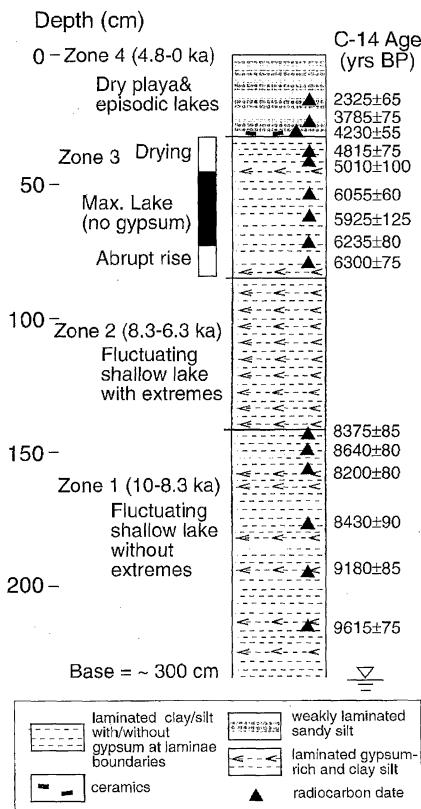


Fig. 2. Four stratigraphic zones of the Holocene deposits of Lake Lunkaransar. Detailed documentation of the cores is available at www.sciencemag.org/feature/data/985056.shl. There is not much difference between our dates and Singh's (4) three dates. The use of depositional rates led him and others to a different chronology.

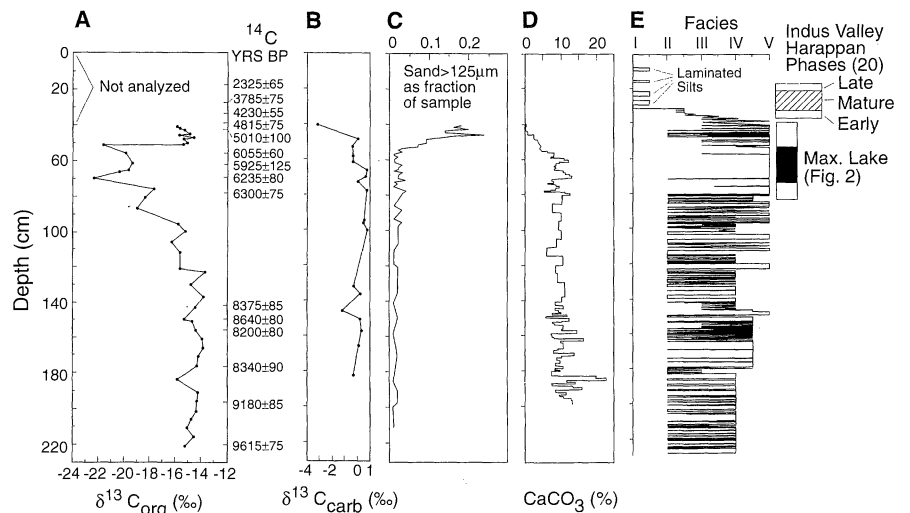


Fig. 3. δ¹³C of organic matter (A) and of the carbonates (B). Grains coarser than 125 μm are shown as a fraction of the total sample (C). (D) Percent CaCO₃. Note the increase and decrease in the sand fraction and CaCO₃, respectively, during 5500 to 4800 yr B.P. Occurrence of the various sedimentary facies along the core (E) can be interpreted as a relative lake depth. The only zone without gypsum in Fig. 2 is reflected here in a continuous facies V. Zone 4 was not analyzed because it represents present-day playa conditions and destroyed primary sedimentary structures.

ports the suggested depth increase and the dilution of the water.

The final decline of the lake high stand was associated with many minor lake-level fluctuations and an increase in eolian sand coarser than 125 μm (Fig. 3C) and containing subangular quartz grains derived from the surrounding dunes. This increase in sand coincides with a decrease in the CaCO_3 percentage and the presence of broken, reworked calcic concretions from soil horizons developed in eolian sands. The increased transport of material from the dunes indicates destabilization of the surfaces of the dunes. No similar input of sand into the lake basin occurred during the previous 5000 years. This sudden pulse of eolian sand implied that there was a major environmental change in the surrounding dune field that is unprecedented in the earlier Holocene.

Our data indicate that the environment and climate of the past 5000 ^{14}C years were similar to those of the present. This long period of relatively low water table was punctuated by a few episodes of inundation of the dry bed of the playa lake as shown by the thin beds of weakly laminated fine silt observed in zone 4; two of these beds are dated at 3785 ± 75 and 2325 ± 65 ^{14}C yr B.P. None of these beds are lacustrine deposits, which may indicate short episodes of heavy rains during a few consecutive years.

The lack of evidence for secondary playa processes that destroyed the laminated deposits and the dates from Lunkaransar indicate that a middle Holocene lake existed from 6300 to 4800 ^{14}C yr B.P., and that the highest lake stand probably ended before 5000 B.P. and not 3500 B.P., as previously suggested (4). The record implies that Lunkaransar lake rose abruptly around 6300 ^{14}C yr B.P. (5000 B.C.), persisted with minor fluctuations for the following 1000 calendar years, fell abruptly to the range of 10 to 40 cm of water at about 5500 ^{14}C yr B.P. (4200 B.C.), and dried completely by 4800 ^{14}C yr B.P. (3500 B.C.). A zone of ceramics and associated charcoal indicates that humans occupied the dry lake bed by 4230 ± 55 ^{14}C yr B.P. (2894 to 2643 B.C.) (Fig. 2). Therefore, the final drying occurred earlier than 4200 B.P. Extrapolation from the deposition rates of the lacustrine phase to the boundary between zone 3 and zone 4 indicates that the final drop of the water table below the surface occurred around 4600 B.P.

This drying phase precedes by 800 to 1000 years the rise of the Early and Mature Harappan phases of the Indus civilization from 4100 to 3500 ^{14}C yr B.P. (2600 to 2000 B.C.) (19) (Fig. 3). This contradicts the climate-culture hypothesis for northwestern India and Pakistan (8, 9). Improved climatic conditions did not lead to the rise of this major urban civilization, as has been suggested (8, 9). The collapse of the Indus culture in 3400 to 3300 ^{14}C yr B.P. (1700 to 1900 B.C.) has been attributed to a change to a

more arid climate at the end of the middle Holocene wet period (4, 8, 9). Our chronology indicates that there is no relation between the proposed drought that caused the desiccation of the lakes and the collapse of the Indus culture, as the lakes dried out >1500 years earlier. The wet climate-Indus civilization relationship was previously challenged (20), but it remains a prime example of a climate-civilization relationship [p. 208 in (9)]. The Indus civilizations flourished mainly along rivers (20) during times when northwestern India experienced semiarid climatic conditions that are similar to those at present.

A few paleoclimate records from the Arabian Sea indicate an increase in the southwestern monsoon activity 10,000 to 9500 years ago. These records also show the decade- to century-scale variations observed in Lunkaransar and that the monsoon weakened about 5500 B.P. (1, 2). The Lunkaransar lacustrine record shows a simultaneous weakening of the monsoon on the Indian subcontinent, which is atmospherically downstream of the Arabian Sea during the southwestern monsoon. However, the contrast in the nature of the early Holocene and the middle Holocene lacustrine phases in Lunkaransar indicates that the hydrological conditions, and therefore the rainfall input, were different then. These differences are supported by records from southeastern Arabia (21). Two observations support the idea that an additional source of water beyond the summer monsoon precipitation is required to produce a perennial lake in Lunkaransar. First, the supposedly maximum summer monsoon rains (7) of the early Holocene were not able to maintain a perennial lake in Lunkaransar, such as existed 6300 to 4800 ^{14}C yr B.P. Second, none of the lake basins of northwestern India that currently experience 450 to 550 mm of summer monsoon rains sustain perennial lakes; according to pollen analyses (6), this was the amount of precipitation that prevailed in Lunkaransar during the lacustrine phases. Therefore, we postulate that an additional source of rainfall must be identified for explaining the lake rise and stabilization during the middle Holocene. We propose that winter precipitation, which currently accounts for only 20% of total precipitation (10), is a potential source (3-7). Winter precipitation may have a much larger effect on percolation to the subsurface hydrology that feeds the lake than increased monsoon rains alone. The additional winter rains made the critical difference between the early and middle Holocene hydrologic conditions. They eliminated the high-frequency level changes and the drop of water to gypsum deposition range and allowed for a perennial lake during the middle Holocene.

References and Notes

1. J. E. Kutzbach, in *Monsoons*, J. S. Fein and P. L. Stephens, Eds. (Wiley, New York, 1987), pp. 247-267; W. L. Prell and J. E. Kutzbach, *Nature* **360**, 647 (1992); F. Sirocco et al., *ibid.* **364**, 322 (1993).

2. J. Overpeck, D. Anderson, S. Trumbore, W. Prell, *Clim. Dyn.* **12**, 213 (1996).

3. R. J. Wasson, in *Quaternary Environments and Geoarchaeology of India-Rajaguru Vol.*, S. Wadia, R. Korisetar, V. S. Kale, Eds. (Geological Society of India, Bangalore, India, 1995) pp. 22-35.

4. G. Singh, R. D. Joshi, A. B. Singh, *Quat. Res.* **2**, 496 (1972); G. Singh, R. D. Joshi, S. K. Chopra, A. B. Singh, *Philos. Trans. R. Soc. London Ser. A* **267**, 467 (1974); G. Singh, R. J. Wasson, D. P. Agarwal, *Rev. Palaeobot. Palynol.* **64**, 351 (1990).

5. R. J. Wasson, G. I. Smith, D. P. Agarwal, *Palaeogeogr. Palaeoclimatol. Palaeoecol.* **46**, 345 (1984).

6. R. A. Bryson and A. M. Swain, *Quat. Res.* **16**, 135 (1981); A. M. Swain, J. E., Kutzbach, S. Hastenrath, *ibid.* **19**, 1 (1983); R. A. Bryson, *Clim. Dyn.* **3**, 169 (1989).

7. J. E. Kutzbach and A. F. Street-Perrott, *Nature* **317**, 130 (1985); COHMAP, *Science* **241**, 1043 (1988); N. Roberts and H. E. Wright Jr., in *Global Climates Since the Last Glacial Maximum*, H. E. Wright et al., Eds. (Univ. Of Minnesota Press, Minneapolis, MN, 1993) pp. 194-220; B. Qin and G. Yu, *Global Planet. Change* **18**, 54 (1998).

8. G. Singh, *Archeol. Phys. Anthropol. Oceania* **6**, 177 (1971); B. Allchin and R. Allchin, *The Rise of Civilization in India and Pakistan* (Cambridge Univ. Press, London, 1982).

9. R. Allchin and B. Allchin, *Origins of a Civilization* (Viking-Penguin India, New Delhi, 1997).

10. The maximum lake area of the present-day Lunkaransar dry lake was about 5 km². The climate is arid with 200 mm of rainfall during the monsoon (June to September) and 40 mm during winter (October to February). Mean monthly temperatures are 35°, 31°, and 15° to 17°C during the premonsoon, monsoon, and winter, respectively. Potential evaporation is >2000 mm/year (197 and 53 mm in August and January, respectively).

11. R. J. Wasson, et al., *Z. Geomorphol. Suppl. B* **45**, 117 (1983); currently, the amount of dust is positively correlated with seasonal monsoon rainfall; A. Krishnan, in *Desertification and Its Control*, P. L. Jaiswal, Ed. (ICAR, New Delhi, 1977) pp. 42-57.

12. B. F. Jones and E. Galan, in *Reviews in Mineralogy*, Vol. 79, S. W. Baily, Ed. (Mineralogical Society of America, Washington, DC, 1988) pp. 631-674; A. Singer, in J. B. Dixon and S. B. Weed, Eds. (Soil Science Society of America, Madison, WI, 1989) pp. 829-872.

13. B. D. Allen, *N.M. Bur. Mines Miner. Res. Bull.* **137**, 166 (1991); _____ and R. Y. Anderson, *Science* **260**, 1920 (1993).

14. Preparation of CO₂ was from organic carbon according to Northfelt et al. and Ramesh et al. [D. W. Northfelt et al., *Geochim. Cosmochim. Acta* **45**, 1895 (1981); R. Ramesh et al., in *Science and Archeology: Proceedings of the Conference on the Applications of Scientific Techniques to Archeology*, Glasgow, UK, 1987, E. A. Slater and J. O. Tate, Eds. (BAR British Series, vol. 196, 1988), p. 591.

15. B. Lazar and J. Erez, *Geology* **18**, 1191 (1990); *Geochim. Cosmochim. Acta* **56**, 335 (1992); N. Gazit-Yaari, thesis, Hebrew University, Jerusalem (1999).

16. P. Baertschi, *Helv. Chim. Acta* **53**, 1030 (1952); H. Craig, *Geochim. Cosmochim. Acta* **3**, 53 (1953).

17. The $\delta^{13}\text{C}_{\text{carb}}$ value of authigenic carbonate is about 2 per mil higher than $\delta^{13}\text{C}_{\text{DIC}}$; thus, the isotopic composition of authigenic carbonates should follow the isotopic composition of the water. However, it is impossible to pick the authigenic carbonate out of a large fraction of eolian carbonates (weathered carbonates with $\delta^{13}\text{C}_{\text{org}}$ of about 0 per mil). It is reassuring that at 8500 yr. B.P. the $\delta^{13}\text{C}_{\text{carb}}$ peak in Fig. 3B is -1.5 per mil, indicating authigenic component of about 30%.

18. The relationship between lake level and $\delta^{13}\text{C}_{\text{DIC}}$ was determined in field and laboratory experiments (16) with MMC from Solar Lake, northern Gulf of Aqaba. Changes in DIC and $\delta^{13}\text{C}_{\text{DIC}}$ as a response to MMC photosynthesis were measured. Laboratory experiments were conducted in aquaria containing MMC and brines with depth (Z) ranging between 5 and 20 cm, and field observations were conducted from depths of 5 to 40 cm. The experiments demonstrated that $\delta^{13}\text{C}$ depletion of the brine was caused by invasion of atmospheric CO₂ into brine depleted in DIC because of intense microbial mat community

(MMC) photosynthesis. Measurements of MMC net productivity (NP) and DIC budgets under different conditions enabled determination of the depletion factor (Φ), which is defined as

$$\Phi[d^{-1}] = \frac{NP[\text{mol}\cdot\text{m}^{-2}\cdot\text{d}^{-1}]}{\text{DIC}[\text{mol}\cdot\text{m}^{-3}]\overline{Z}[\text{m}]}$$

and has units of per day. The observations showed that the onset of $\delta^{13}\text{C}$ depletion was when $\Phi \sim 0.2$ per day. Substituting this value of Φ into the equation together with the normal values for MMC net production (250 mg of C per square meter per day) and DIC concentration (1 to 4 mmol/l) yield an estimate for maximum lake depth (Z) during low stand of 10 to 40 cm.

19. G. L. Possehl, in *South Asian Archeology 1991*, A. Gail and G. Mevissou, Eds. (Steiner Verlag, Stuttgart, 1993), pp. 231–250.
20. Vishnu-Mittre, *Geophytology* 4 (no. 1), (1974); *Pa-leobotanist* 25, 549 (1978); V. N. Misra, in *Frontiers of the Indus Civilization*, B. B. Lal and S. P. Gupta, Eds. (Books and Books, New Delhi, 1984), pp. 461–489; B. K. Thapar, *Recent Archeological Discoveries in India* (The Centre for East Asian Cultural Studies, United Nations Educational, Scientific and Cultural Organization, 1995); M.-A. Courty, in *Ancient People and Landscape*, E. Johnson, Ed. (Texas Univ. Press, Lubbock, 1995), pp.105–126.
21. S. J. Burns, A. Matter, N. Frank, A. Mangini, *Geology* 26, 499 (1998).

22. M. Stuiver and P. J. Reimer, *Radiocarbon* 35, 215 (1993).
23. Supported by National Science Foundation (NSF) grants EAR-9104489 and EAR-9417896 to V.R.B. and EAR-9418989 to L.L.E. Additional support to L.L.E. was provided by NSF Post-Doctoral Fellowship grant EAR-9202498, conducted at the Earth System Science Center, Pennsylvania State University. ^{14}C analyses were conducted at and partially funded by the NSF, University of Arizona AMS laboratory. We thank A. K. Singhvi for fruitful discussions. M. Shmida helped with drafting and I. Zicha with laboratory analyses.

4 September 1998; accepted 26 February 1999

Clinoenstatite in Alpe Arami Peridotite: Additional Evidence of Very High Pressure

K. N. Bozhilov, H. W. Green II, L. Dobrzhinetskaya

Observations by transmission electron microscopy show that lamellae of clinoenstatite are present in diopside grains of the Alpe Arami garnet lherzolite of the Swiss Alps. The simplest interpretation of the orientation, crystallography, and microstructures of the lamellae and the phase relationships in this system is that the lamellae originally exsolved as the high-pressure C-centered form of clinoenstatite. These results imply that the rocks were exhumed from a minimum depth of 250 kilometers before or during continental collision.

In fresh samples of the Alpe Arami garnet lherzolite of the Swiss Alps, the oldest generation of olivine contains up to 1% by volume rod-shaped precipitates of FeTiO_3 parallel to [010] of olivine and up to $\sim 0.2\%$ by volume tabular chromite precipitates parallel to (100) (1). These oxide precipitates are much more abundant than reported previously (2) and suggest much greater solubility of highly charged cations than has been measured in mantle olivine (3). These precipitates are older than the dislocation microstructure (4) and therefore predate the Alpine deformation. This older generation of olivine exhibits a unique lattice-preferred orientation (LPO) (5) that is incompatible with the deformation mechanisms known to operate in olivine in other naturally deformed peridotites (6) and in the laboratory (7). Partial recrystallization during Alpine deformation of this peridotite has produced a younger generation of olivine that contains no oxide inclusions, a normal LPO associated with a new foliation, and a normal dislocation substructure (5). These observations led Dobrzhinetskaya *et al.* (1) to infer an extreme depth of origin (>300 km) of the peridotite, a proposition that has been controversial because the high TiO_2 contents of the olivine inferred from volume fraction measurements of the precipitates could not be confirmed by broad-beam electron micro-

probe measurements (8). Here we confirm an earlier report of clinoenstatite lamellae exsolved from diopside in these rocks (9). Detailed analysis of these lamellae indicates that the phase originally precipitated was probably the high-pressure monoclinic polymorph of enstatite, which is stable only at depths exceeding 250 km at upper mantle temperatures.

Twenty diopside crystals from specimens that also contain olivine exhibiting extensive precipitation of oxides were chosen for examination by analytical transmission electron microscopy (TEM) (10). The diopsides were selected from two microenvironments: within and adjacent to garnets and scattered in the olivine + enstatite matrix. The latter group of diopsides shows a nearly perfect substructure other than widely spaced retrograde lamellae of amphibole (11). The former exhibit abundant clinoenstatite lamellae and ubiquitous thin (010) amphibole slabs (Fig. 1, A and B) (12). Locally, these diopsides also contain numerous chromite exsolution lamellae and rare orthoenstatite lamellae (11). The density of clinoenstatite lamellae varies from about 1 to 5% by volume (Fig. 1A).

The clinoenstatite lamellae [space group (SG) $P2_1/c$] and diopside host (SG $C2/c$) share the b axis, with their c axes subparallel at an angle of about 2° (Fig. 1D). The lamellae are oriented approximately parallel to (401) of diopside, making an angle of 20° to 24° with the (100) planes of both phases (Figs. 1C). Bright-field images exhibit blotchy contrast within the

lamellae on a wavelength of a few nanometers, which is not observed in the diopside host (Fig. 1C). Darkfield imaging of the lamellae with $h + k = \text{even}$ reflections shows the same mottling; alternating darker and lighter contrast regions are elongated across the lamellae (Fig. 2A). In contrast, imaging with $h + k = \text{odd}$ shows generally equidimensional domains that are smaller and exhibit much higher contrast (Fig. 2B). High-resolution TEM (HRTEM) imaging down the b axis (Fig. 3) clearly shows that the contrast is mottled within the lamella and that the spacing between (100) planes of the primitive lattice of the clinoenstatite lamella is 9 \AA (SG $P2_1/c$) as compared to the $\sim 4.5 \text{ \AA}$ lattice fringes in diopside (SG $C2/c$). Examination of Fig. 3 also shows that the dark/light mottled contrast that was visible in both brightfield and $h + k = \text{even}$ imaging is a result primarily of elastic distortion of the lattice. Closer examination, however, shows numerous places where the (100) lattice fringes are systematically offset by $a/2$. Many of these sites of lattice offset are at the margins of the regions of alternating contrast, but others do not show such correlation (13). The arrays of lattice terminations generally border domains with apparent $\sim 4.5 \text{ \AA}$ spacing rather than forming sharply defined interfaces. These could be either true relict domains of $C2/c$ pyroxene or, more likely because of their small size, regions where the surfaces of lattice offset are inclined with respect to the beam direction [010], causing partial overlap of neighboring domains. These observations, coupled with the marked differences in darkfield imaging with $h + k = \text{odd}$ or even, are consistent with the interpretation that regions of lattice fringe offset constitute antiphase boundaries, and the regions between them are antiphase domains related by displacement vector $1/2(a + b)$. Examination of the interfaces between lamellae and host on all scales shows that they lack misfit dislocations; they exhibit crystallographically controlled steps accompanied by small adjustments of the lattice fringes as they cross the boundary (Fig. 3). Thus, the boundaries are coherent.

The compositions of the studied crystals as determined by analytical electron microscopy are as follows: host diopside, $(\text{Ca}_{0.94}\text{Na}_{0.06}\text{Mg}_{0.84}\text{Fe}_{0.08}\text{Cr}_{0.03}\text{Al}_{0.04}\text{Ti}_{0.01})-$

Institute of Geophysics and Planetary Physics and Department of Earth Sciences, University of California, Riverside, CA 92521, USA.